

Published in final edited form as:

Chem Sci. 2014 February 1; 5(2): . doi:10.1039/C3SC52777H.

Synthesis of Bioinspired Carbohydrate Amphiphiles that Promote and Inhibit Biofilms

Eric L. Dane^a, Alicia E. Ballok^b, George A. O'Toole^b, and Mark W. Grinstaff^a

Mark W. Grinstaff: mgrin@bu.edu

^aDepartments of Chemistry and Biomedical Engineering, Boston University, Boston, MA

^bDepartment of Microbiology & Immunology, Geisel School of Medicine at Dartmouth, Hanover, NH

Abstract

The synthesis and characterization of a new class of bioinspired carbohydrate amphiphiles that modulate *Pseudomonas aeruginosa* biofilm formation are reported. The carbohydrate head is an enantiopure poly-amido-saccharide (PAS) prepared by a controlled anionic polymerization of β -lactam monomers derived from either glucose or galactose. The supramolecular assemblies formed by PAS amphiphiles are investigated in solution using fluorescence assays and dynamic light scattering. Dried samples are investigated using X-ray, infrared spectroscopy, and transmission electron microscopy. Additionally, the amphiphiles are evaluated for their ability to modulate biofilm formation by the Gram-negative bacterium *Pseudomonas aeruginosa*. Remarkably, from a library of eight amphiphiles, we identify a structure that promotes biofilm formation and two structures that inhibit biofilm formation. Using biological assays and electron microscopy, we relate the chemical structure of the amphiphiles to the observed activity. Materials that modulate the formation of biofilms by bacteria are important both as research tools for microbiologists to study the process of biofilm formation and for their potential to provide new drug candidates for treating biofilm-associated infections.

Introduction

Amphiphiles containing a hydrophilic carbohydrate headgroup and a hydrophobic tail play a variety of essential biological roles.¹ Studies examining the effect of oligo- and polysaccharide headgroup on assembly and bioactivity have highlighted the importance of carbohydrate-carbohydrate interactions in the assembled structures.²⁻¹⁰ As seen in natural and synthetic systems, self-assembled structures may possess unique or increased bioactivity in comparison to their individual, unassembled building blocks.¹¹⁻¹³ Therefore, the ability to prepare a wide-range of carbohydrate amphiphiles that display variations in assembly is a promising route to dynamic, bioactive structures. However, glycolipids containing oligo- or polymeric headgroups can be challenging to prepare by traditional synthetic means¹⁴ despite recent advances in carbohydrate chemistry.¹⁵⁻¹⁷ Recognizing this need, we describe a synthetic strategy to prepare bioinspired poly-amido-saccharide (PAS)^{18, 19} amphiphiles that offer many potential structures that are readily accessible through monomer and initiator selection. Specifically, we report the synthesis of eight new polymeric amphiphiles (Fig. 1) that form supramolecular assemblies in aqueous solution. Additionally, we report the ability

of PAS amphiphiles to modulate biofilm formation of *Pseudomonas aeruginosa*, a Gram-negative bacterium known to cause biofilm-associated infections.

Biofilms are surface-adhered bacterial communities surrounded by an extracellular matrix.²⁰ In biofilms, pathogenic bacteria become more tolerant to antibiotic treatment and the host immune response.²⁰ The ability to influence biofilm formation selectively, without affecting the bacterial growth rate, is important for studying the mechanisms that govern biofilm formation. Additionally, the ability to inhibit biofilm formation provides opportunities to develop new therapies for biofilm-associated illness. It has been shown that synthetic amphiphilic macromolecules^{21–27}, including those inspired by antimicrobial peptides^{28–31}, can exhibit potent and selective activity against a variety of microbes.³² Given that carbohydrate amphiphiles, such as lipopolysaccharide and rhamnolipids, play important roles in bacterial communities, we reasoned that *P. aeruginosa* would be an excellent model organism to explore the bioactivity of PAS amphiphiles.³³

PASs are enantiopure synthetic polymers containing sugar-derived repeat units joined by an amide bond.¹⁸ Herein, we use a polymerization initiator that contains one or two palmitamide chains, derived from the saturated long-chain fatty acid palmitic acid, to synthesize PAS amphiphiles (Fig. 2) in a two-step process - polymerization followed by deprotection. Using this approach, a set of amphiphilic macromolecules are prepared that vary in three important ways: (1) the “a-group” of compounds has a single palmitamide chain joined to the PAS polymer by a 6-aminohexanoic acid linker, whereas the “b-group” has two palmitamide chains joined to the PAS polymer by an L-lysine linker; (2) the **1**-series has a headgroup synthesized from only galactose(gal)-derived monomers, whereas the **2**-series has a headgroup formed by the random copolymerization of a 1:1 mixture of gal- and glucose(glc)-derived polymers; and (3) two lengths of headgroup are prepared, one with a theoretical degree of polymerization (DP_{th}) of 10 and one with a DP_{th} of 20.

Results and Discussion

PAS Amphiphile Synthesis and Characterization

Our synthetic approach to PAS amphiphiles relies on the controlled anionic ring-opening polymerization of a β -lactam monomer^{34, 35}, specifically monomers **3** (gal-derived) and **4** (glc-derived) (Fig. 2), both of which are prepared via a one-step procedure.³⁶ The polymerization is initiated by pentafluorophenol ester **5** or **6**, which have one or two palmitamide chains, respectively. Amphiphiles with DP_{th} 's of 10 and 20 were prepared by using either 10 or 5 mol% of initiator, respectively. After polymerization, the benzyl ether protecting groups were removed using sodium metal in liquid ammonia and the deprotected polymers were purified by dialysis. The yields, reported over both steps, ranged from 71–96%.

All the protected amphiphiles were characterized using ¹H- and ¹³C-NMR. Due to the polymeric structure, the NMR spectra were broadened. The molecular weights of the protected amphiphiles were determined using gel permeation chromatography (GPC) (Table S1[†]). The M_n -values were in good agreement with the theoretical values and the measured dispersities (\bar{M}_w/\bar{M}_n) were between 1.1 and 1.2.

Following deprotection, the amphiphiles were characterized using ¹H-NMR and IR. DPs were estimated using ¹H-NMR integrations and were in good agreement with theoretical values (Table S2[†]). The molecular weights of amphiphiles, **1b₂₀**, **2a₁₀**, and **2a₂₀**, were

[†]Electronic Supplementary Information (ESI) available: Experimental procedures, supplementary tables, figures, and NMR spectra. See DOI: 10.1039/b000000x/

confirmed using MALDI-tof and were found to be in good agreement with the theoretical mass of the sodium adduct and showed the expected spacings of 189 amu between species with different DPs (Fig. S1[†]). Because of their amphiphilic nature and propensity to assemble, the deprotected amphiphiles were not characterized by GPC. However, we have previously shown that deprotection has no adverse effect on PAS molecular weight.^{18, 19}

Characterization of Supramolecular Assemblies

The critical micelle concentrations (CMC) of the amphiphiles were determined by monitoring pyrene fluorescence (Fig. 2, far right).³⁷ However, amphiphiles **1a**₁₀, **1a**₂₀, and **1b**₁₀ formed aggregates that readily precipitated, making it difficult to accurately measure the CMC using this method. Noticeable precipitate could be observed by eye at concentrations as low as 1 μM, and therefore we report this as an upper bound. The other amphiphiles formed visibly clear, stable suspensions in water and phosphate buffered saline (PBS), and the values are reported for PBS. The general understanding of how amphiphile structure affects CMC is that increasing the hydrophilic headgroup size relative to the hydrophobic tail size raises the CMC, and vice versa. Based on the CMCs measured, the **1**-series does not behave as a typical amphiphile. Hato *et al.* commented that certain oligosaccharide headgroups can engage in attractive carbohydrate-carbohydrate interactions that cause them not to behave as typical hydrophilic groups, as appears to be the case with the **1**-series but not with the **2**-series.³ The **2**-series follows the trends generally observed for amphiphiles. The CMC of **2a**₂₀ (36 μM) is significantly higher than **2a**₁₀ (20 μM), hence for **2a** increasing the hydrophilic portion of the amphiphile decreases its tendency to assemble in solution. The CMC values for **2b**₁₀ and **2b**₂₀ are similar, suggesting that increasing the PAS headgroup length has less effect when the endgroup is more hydrophobic. As would be expected for a typical amphiphile, increasing the number of fatty acid chains in the tail of the **2**-series amphiphiles decreases the CMC, as evidenced by comparing the CMCs of the **a**-group (1 chain) to the **b**-group (2 chains).

The turbidity of the dispersions (1 mg/mL) formed by **1b**₂₀, **2a**₁₀, **2a**₂₀, **2b**₁₀, and **2b**₂₀ was monitored at room temperature and at 37 °C by recording the absorbance due to scattering at 330 nm (Fig. S2[†]). Only **1b**₂₀ showed additional assembly into larger structures, which are more effective at scattering light. Heating to 37 °C was required for this process to occur in a timespan of hours, as **1b**₂₀ did not show increased scattering within the first 30 hours at room temperature.

To investigate the size of the aggregates formed by the dispersible amphiphiles, the apparent hydrodynamic diameter (D_h) was determined by dynamic light scattering (DLS) in PBS buffer at an amphiphile concentration of 1.0 mg/mL. In general, the amphiphiles showed nanoscale assemblies that are relatively heterogeneous based on the measured polydispersities. Amphiphile **1b**₂₀ initially displayed small structures with a diameter of 34 nm. After incubation of the sample at 37°C for 16 hours the size of the structures increased 3-fold to 105 nm.

To examine the crystalline order of the assemblies, we performed wide-angle X-ray scattering (WAXS) on powder samples prepared by lyophilizing flash-frozen aqueous suspensions of the amphiphiles at concentrations above the CMC (Fig. 3). The amphiphiles that were the least dispersible (**1a**₁₀, **1b**₁₀, and **1a**₂₀) produced the most structured patterns. Focusing on these amphiphiles, we can observe correlations between the molecular structure of the amphiphile and the crystalline order observed in the aggregates. The fact that **1a**₁₀ and **1b**₁₀ show similar diffraction patterns with consistent d-spacings suggests that the crystalline order observed resides in the gal-derived PAS headgroup, which is the same in both, rather than the hydrophobic tail, which differs significantly between the two species.

The hydrophobic tails may have crystalline order, but as they comprise a relatively small part of the molecule it is difficult to discern from the WAXS patterns. Additionally, the peaks appear more intense in **1a₁₀** compared to **1b₁₀**, suggesting that a tail with a single palmitamide promotes order relative to a tail with two fatty acid chains. Comparing **1a₁₀** to **1a₂₀** suggests that a shorter headgroup ($DP_{th}=10$) promotes order relative to a longer headgroup ($DP_{th}=20$). In contrast to **1a₁₀**, **1b₁₀**, and **1a₂₀**, the amphiphiles that formed stable suspensions gave WAXS patterns without defined peaks. The **2**-series all gave similar, unstructured patterns, hence only a single representative profile (**2a₁₀**) is shown in Fig. 3.

To further understand the relationship between the **1**-series and **2**-series, we focus on the amphiphiles with $DP_{th}=10$. The fact that **2a₁₀** and **2b₁₀** show no defined scattering peaks, whereas **1a₁₀** and **1b₁₀** show clear crystalline order, highlights the importance of carbohydrate stereochemistry on assembly. Amphiphiles **1a₁₀** and **2a₁₀** are structurally the same except that the stereochemistry at the 4-position (see Fig. 1, purple dashed oval) of the pyranose ring has been randomly varied in **2a₁₀**; the same relationship exists between **1b₁₀** and **2b₁₀**. Therefore, we conclude that the PAS amphiphiles with headgroups composed only of gal-derived repeat units can pack into an ordered, partially crystalline assembly, and that this packing is prevented by the introduction of disorder in the form of a headgroup made of a random copolymer.

Amphiphile **1b₂₀** appears to violate the trend of ordered packing in the PAS headgroup displayed by the **1**-series, given that its WAXS pattern was more similar to that of the **2**-series amphiphiles. However, the increased turbidity observed in dispersions of **1b₂₀** upon heating could be caused by the amphiphiles rearranging into a more ordered assembly. Therefore, we lyophilized a dispersion of **1b₂₀** after incubation in PBS at 37 °C for 16 hours followed by dialysis, and were able to observe subtle diffraction peaks (Fig. 3, red arrows) that correspond with the major peaks of **1a₁₀**, **1b₁₀**, and **1a₂₀**, indicating that the crystalline order increased with incubation. We suggest that **1b₂₀** forms assemblies with ordered PAS headgroups more slowly than other **1**-series members because it contains two fatty acid chains and has a $DP_{th}=20$, two structural factors that appear to disfavor ordered headgroups in this system.

The powder samples used for WAXS were also investigated by IR, and **1a₁₀** and **1b₁₀** gave spectra with sharper bands in comparison to the other amphiphiles (Fig. 3B, Fig. S3[†] for all spectra). In contrast to WAXS, IR does not directly examine crystalline order, however the narrowing of bands among spectra of similar samples is understood to result from an increase in structural order. We observe that in the region of the OH and NH stretches (yellow), **1a₁₀** and **1b₁₀** show evidence of ordered H-bonding based on the structure of the band and a shift to lower energy. A comparison of the spectrum of **1b₂₀** before and after incubation at 37 °C (**1b₂₀***) confirms an increase in order, as was observed with WAXS. The amide-I band (orange) occurs in the range of 1665–1675 cm^{-1} and the amide-II band (green) shifts to lower energies and splits into two bands in the more crystalline samples (see **1a₁₀**, **1b₁₀**, and **1b₂₀***). For peptides, the amide-I and amide-II bands can be used to evaluate the amount and type of hydrogen bonding. However, we are hesitant to make such interpretations in the spectra of PASs because they contain a hemiamidal structure that may not obey the trends seen in peptides. Nonetheless, the IR spectra of **1a₁₀** and **1b₁₀** support the conclusion that the carbohydrate headgroups are ordered, and confirm that carbohydrate-carbohydrate interactions, such as hydrogen bonding, are playing an important role in aggregate formation.

Finally, we used transmission electron microscopy (TEM) to visualize the assemblies formed by the PAS amphiphiles. TEM micrographs of **1b₂₀**, **2a₁₀**, and **2a₂₀** are shown in Fig. 4 and additional micrographs of the other amphiphiles are available as supplementary

information, Fig. S4[†]. Amphiphiles **1a₂₀**, **2a₁₀** (Fig. 4C), **2a₂₀** (Fig. 4D), and **2b₂₀** appeared as globular micellar aggregates with diameters less than 100 nm. In contrast, the assemblies of **1b₁₀** and **2b₁₀** were elongated worm-like micelles. Interestingly, **1b₂₀** transformed from a globular aggregate (Fig. 4A) to a worm-like aggregate (Fig. 4B) following incubation for 16 hrs at 37°C based on the TEM micrographs. Amphiphile **1a₁₀**, the most structured based on WAXS, appeared as particles with an unusual internal structure. The observation that **1b₁₀** and **2b₁₀** form worm-like micelles can be rationalized based on the larger **b**-group tail promoting less curvature. In the case of **1b₂₀**, we conclude that the transition from a globular to worm-like micellar state results from better packing of the headgroups following incubation at 37°C. As the headgroups pack more closely they are less hydrated and therefore require less space, thus promoting the transition to a structure with less curvature.

***Pseudomonas aeruginosa* Biofilm Modulation**

The amphiphiles that formed stable suspensions (**1b₂₀**, **2a₁₀**, **2a₂₀**, **2b₁₀**, **2b₂₀**) were tested for their ability to influence biofilm formation by *P. aeruginosa* strain PA14³⁸, a clinical isolate with high virulence. Biofilm formation was quantified using a previously described assay that measures crystal violet absorbance at 550 nm to assess surface-attached biomass.³⁹ Amphiphiles **2a₁₀** and **2a₂₀** showed similar abilities to inhibit biofilm formation (Fig. 5). In contrast, **1b₂₀** promoted biofilm formation, and it was found that to reliably observe this activity, the stock solution of **1b₂₀** (4 mg/mL) had to be incubated at 37 °C overnight. Amphiphiles **2b₁₀** and **2b₂₀** showed little activity (not shown). The activity of **1b₂₀**, **2a₁₀**, and **2a₂₀** was concentration dependent, with **1b₂₀** showing biofilm promotion at and above 0.50 mg/mL and **2a₁₀** and **2a₂₀** showing biofilm inhibition at and above 0.25 mg/mL. Bacterial growth, measured in a separate assay, was not significantly affected by **1b₂₀**, **2a₁₀**, and **2a₂₀** at their active concentrations (Fig. S5[†]). In addition, the corresponding PAS gal-derived homopolymer and 1:1 random copolymer of a similar molecular weight, but lacking the hydrophobic endgroup, showed no activity in either the biofilm or growth assays, confirming that the amphiphilic structure is essential to the observed bioactivity (not shown). Because the active amphiphiles show activity at concentrations significantly above their CMC and because the headgroups lacking a hydrophobic tail are inactive, we conclude that the supramolecular assemblies are important for the observed bioactivity.

In exploring the mechanism by which **2a₁₀** and **2a₂₀** inhibit biofilm formation, we considered two possibilities. First, given our previous observation that rhamnolipid surfactants produced by *P. aeruginosa* can inhibit biofilm formation, we explored the possibility that **2a₁₀** and **2a₂₀** act as surfactants.³³ It is understood that rhamnolipids disrupt biofilm formation by affecting cell-surface and cell-cell interactions³³ by forming assemblies that lower the surface tension of water at interfaces.⁴⁰ To evaluate the surfactant properties of the dispersible PAS amphiphiles reported here, we measured their effect on surface tension using a hanging drop assay (Fig. S6[†]). At a concentration of 1.0 mg/mL in PBS buffer, both **2a₁₀** and **2a₂₀** significantly lowered the surface tension in comparison to PBS buffer. In contrast, **1b₂₀**, **2b₁₀**, and **2b₂₀** displayed no or little ability to decrease the surface tension. Many amphiphiles act as surfactants,⁴¹ however amphiphiles of the **b**-group are significantly less effective at lowering the surface tension of water relative to amphiphiles of the **a**-group based on our measurements. As **2b₁₀** and **2b₂₀** share the same headgroup as **2a₁₀** and **2a₂₀**, we conclude that the additional palmitamide chain in the **b**-group tail is responsible for the lack of surfactant activity, and thus, their lack of activity at inhibiting biofilm formation. To further confirm that **2a₁₀** and **2a₂₀** are mimicking the surfactant activity of rhamnolipids, we tested whether they also promote bacterial swarming motility. Swarming motility is a process by which *P. aeruginosa* move across a semi-solid surface, and it requires that the bacterium produce its own rhamnolipid surfactant to lower the surface tension of water at the surface.⁴² Using a plate-based assay, **2a₁₀** (Fig. 5) and

2a₂₀ (not shown) rescued swarming motility in a rhamnolipid deficient mutant (*rhlA*). Thus, **2a₁₀** and **2a₂₀** mimic the surfactant activity of rhamnolipid under these conditions, further supporting our hypothesis that the mechanism of biofilm inhibition is related to their surfactant properties. A second possibility was that **2a₁₀** and **2a₂₀** reduced levels of c-di-GMP, an intracellular signaling molecule required for biofilm formation in *P. aeruginosa*.⁴³ However, no difference in c-di-GMP levels in bacteria treated with the active amphiphiles (**1b₂₀**, **2a₁₀**, and **2a₂₀**) compared to PBS-treated controls was observed (not shown).

The ability of **1b₂₀** to promote biofilm formation was unexpected. Galactose was chosen for investigation because other galactose containing structures, such as dendrons, have shown the ability to inhibit biofilm formation in *P. aeruginosa* by interaction with a bacterial surface lectin.^{44, 45} However, we did not observe this activity in the amphiphiles or in the unassembled polymer headgroups lacking the hydrophobic tail. As we have recently reported, nonamphiphilic gal-derived PASs are not recognized by the gal-specific lectin on the surface of hepatocytes.¹⁹ We suspect that the difference in structure between the gal-derived PAS repeat unit and natural galactose derivatives is large enough to prevent interaction with gal-specific lectins. Additionally, if the activity we observe here resulted from an interaction between PAS gal-residues and bacterial receptors, we would expect to see some level of activity from **2b₁₀** and **2b₂₀**, which have headgroups with half of their repeat units derived from galactose. Therefore, we conclude that a specific interaction between a gal-derived repeat unit and a bacterial surface lectin is likely not responsible for the biofilm promotion activity.

As previously mentioned, the **1b₂₀** suspension requires incubation overnight at 37°C in order to show consistent biofilm promotion. We have demonstrated that larger aggregates with more highly ordered headgroups are formed during incubation at 37°C using turbidity measurements, DLS, WAXS, IR, and TEM. Based on TEM, these aggregates are rod-like extended structures (Fig. 4B). It is known that many bacteria, including *P. aeruginosa*, utilize fibrillar adherence proteins in the process of biofilm formation.⁴⁶ Recently, *B. subtilis*, a Gram positive bacterium, was shown to use endogenously produced amyloid fibers for cell adherence during biofilm formation.⁴⁷ Based on these observations, we suggest that the ordered aggregates of **1b₂₀** may be promoting biofilm formation by an analogous process. Currently, we are working to better understand the specific mechanism of biofilm promotion by **1b₂₀** using a genetic approach that employs mutant screening to elucidate the molecular pathways that are affected.

Conclusions

In summary, we report that PAS amphiphiles containing a headgroup with gal- or gal/glc-derived repeat units form assembled structures in aqueous solution. The assemblies prepared from the **1**-series of polymeric amphiphiles result from hydrophobic interactions between tail groups and attractive interactions between the headgroups, such as hydrogen bonding. In contrast, the random copolymer headgroups of the **2**-series are more hydrated and have more repulsive, and less attractive, interactions. From the WAXS patterns and IR, we gain additional insights about the relationship between the structure and the crystalline order present in the PAS headgroup, specifically: (1) for the **1**-series, the **a**-group (one palmitamide chain) promotes more ordered structures than the **b**-group (two palmitamide chains); (2) for the **1**-series, the amphiphiles with DP_{th}=10 form more ordered structures than those with DP_{th}=20; (3) the **2**-series amphiphiles do not form assemblies with crystalline order in the headgroup because of the disorder introduced by the PAS random copolymer. Amphiphiles **2a₁₀** and **2a₂₀** inhibited biofilm formation of *P. aeruginosa* and rescued swarming in a mutant strain of *P. aeruginosa* unable to produce rhamnolipid biosurfactants, suggesting they are acting via a similar mechanism to rhamnolipids by

lowering the surface tension of water.^{33, 42} In contrast, **1b₂₀** promoted biofilm formation by a mechanism that is related to its ability to form rod-like aggregates and which is under further investigation. The novelty of the structures presented here and their practical synthesis suggest that PAS amphiphiles are a promising new class of bioinspired synthetic glycolipids. Future work is underway to investigate the effect of varying the structure of both the PAS headgroup and the hydrophobic tail to further understand how structure affects assembly and the ability of the assemblies to modulate biofilm formation.

Supplementary Material

Refer to Web version on PubMed Central for supplementary material.

Acknowledgments

We thank Dr. J. Sparks for collecting WAXS patterns and L. Filkins for assistance with the TEM studies. E.L.D. acknowledges receipt of NIH fellowship 1F32GM097781 and G.A.O NIH grant R01AI083256.

references

1. Holst, O. Glycoscience. Fraser-Reid, B.; Tatsuta, K.; Thiem, J., editors. Vol. ch. 39. Berlin Heidelberg: Springer; 2008. p. 1603-1627.
2. Takeoka S, Sou K, Boettcher C, Fuhrhop J-H, Tsuchida E. J. Chem. Soc., Faraday Trans. 1998; 94:2151–2158.
3. Hato M, Minamikawa H, Tamada K, Baba T, Tanabe Y. Ad. Colloid Interface Sci. 1999; 80:233–270.
4. Tanaka M, Schneider MF, Brezesinski G. Chem Phys Chem. 2003; 4:1316–1322. [PubMed: 14714379]
5. Tirelli N. Macromol. Biosci. 2006; 6:575–578. [PubMed: 16868921]
6. Houga C, Giermanska J, Lecommandoux S, Borsali R, Taton D, Gnanou Y, Le Meins J-F. Biomacromolecules. 2008; 10:32–40. [PubMed: 19072234]
7. Birchall LS, Roy S, Jayawarna V, Hughes M, Irvine E, Okorogheye GT, Saudi N, De Santis E, Tuttle T, Edwards AA, Ulijn RV. Chem. Sci. 2011; 2:1349–1355.
8. Upadhyay KK, Le Meins J-F, Misra A, Voisin P, Bouchaud V, Ibarboure E, Schatz C, Lecommandoux S. Biomacromolecules. 2009; 10:2802–2808. [PubMed: 19655718]
9. de Medeiros Modolon S, Otsuka I, Fort S, Minatti E, Borsali R, Halila S. Biomacromolecules. 2012; 13:1129–1135. [PubMed: 22397388]
10. Smith, DK. Supramolecular Chemistry: From Molecules to Nanomaterials. Gale, PA.; Steed, JW., editors. Vol. vol. 7. New York: John Wiley & Sons, Ltd; 2012. p. 3169-3182.
11. Barnard A, Smith DK. Angew. Chem. Int. Ed. 2012; 51:6572–6581.
12. Levine PM, Carberry TP, Holub JM, Kirshenbaum K. Med. Chem. Comm. 2013; 4:493–509.
13. Petkau-Milroy K, Brunsveld L. Org. Biomol. Chem. 2013; 11:219–232. [PubMed: 23160566]
14. Hato M, Minamikawa H. Langmuir. 1996; 12:1658–1665.
15. Hsu C-H, Hung S-C, Wu C-Y, Wong C-H. Angew. Chem. Int. Ed. 2011; 50:11872–11923.
16. Krock L, Esposito D, Castagner B, Wang C-C, Bindschadler P, Seeberger PH. Chem. Sci. 2012; 3:1617–1622.
17. Wang L-X, Davis BG. Chem. Sci. 2013; 4:3381–3394. [PubMed: 23914294]
18. Dane EL, Grinstaff MW. J. Am. Chem. Soc. 2012; 134:16255–16264. [PubMed: 22937875]
19. Dane EL, Chin SL, Grinstaff MW. ACS Macro Lett. 2013:887–890.
20. Costerton JW, Stewart PS, Greenberg EP. Science. 1999; 284:1318–1322. [PubMed: 10334980]
21. Liu D, Choi S, Chen B, Doerksen RJ, Clements DJ, Winkler JD, Klein ML, DeGrado WF. Angew. Chem., Int. Ed. 2004; 43:1158–1162.
22. Chu-Kung AF, Bozzelli KN, Lockwood NA, Haseman JR, Mayo KH, Tirrell MV. Bioconjugate Chem. 2004; 15:530–535.

23. Meyers SR, Juhn FS, Griset AP, Luman NR, Grinstaff MW. *J. Am. Chem. Soc.* 2008; 130:14444–14445. [PubMed: 18842041]
24. Oda Y, Kanaoka S, Sato T, Aoshima S, Kuroda K. *Biomacromolecules.* 2011; 12:3581–3591. [PubMed: 21846110]
25. Papadopoulos A, Shiao TC, Roy R. *Mol. Pharm.* 2011; 9:394–403. [PubMed: 22201286]
26. Xue X, Pasparakis G, Halliday N, Winzer K, Howdle SM, Cramphorn CJ, Cameron NR, Gardner PM, Davis BG, Fernández-Trillo F, Alexander C. *Angew. Chem. Int. Ed.* 2011; 50:9852–9856.
27. Fukushima K, Tan JPK, Korevaar PA, Yang YY, Pitera J, Nelson A, Maune H, Coady DJ, Frommer JE, Engler AC, Huang Y, Xu K, Ji Z, Qiao Y, Fan W, Li L, Wiradharma N, Meijer EW, Hedrick JL. *ACS Nano.* 2012; 6:9191–9199. [PubMed: 22998441]
28. Mowery BP, Lindner AH, Weisblum B, Stahl SS, Gellman SH. *J. Am. Chem. Soc.* 2009; 131:9735–9745. [PubMed: 19601684]
29. Lienkamp K, Tew GN. *Chem. Eur. J.* 2009; 15:11784–11800. [PubMed: 19798714]
30. Lienkamp K, Madkour AE, Tew GN. *Adv. Polym. Sci.* 2011:1–32.
31. Wu H, Niu Y, Padhee S, Wang RE, Li Y, Qiao Q, Bai G, Cao C, Cai J. *Chem. Sci.* 2012; 3:2570–2575.
32. Mintzer MA, Dane EL, O'Toole GA, Grinstaff MW. *Mol. Pharm.* 2011; 9:342–354. [PubMed: 22126461]
33. Davey ME, Caiazza NC, O'Toole GA. *J. of Bacteriol.* 2003; 185:1027–1036. [PubMed: 12533479]
34. Zhang J, Kissounko DA, Lee SE, Gellman SH, Stahl SS. *J. Am. Chem. Soc.* 2009; 131:1589–1597. [PubMed: 19125651]
35. Zhang J, Gellman SH, Stahl SS. *Macromolecules.* 2010; 43:5618–5626.
36. Kału a Z, Abramski W, Beł ecki C, Grodner J, Mostowicz D, Urbanski R, Chmielewski M. *Synlett.* 1994:539–541.
37. Astafieva I, Zhong XF, Eisenberg A. *Macromolecules.* 1993; 26:7339–7352.
38. Rahme L, Stevens E, Wolfort S, Shao J, Tompkins R, Ausubel F. *Science.* 1995; 268:1899–1902. [PubMed: 7604262]
39. O'Toole GA, Kolter R. *Mol. Microbio.* 1998; 28:449–461.
40. Sánchez M, Aranda FJ, Espuny MJ, Marqués A, Teruel JA, Manresa Á, Ortiz A. *J. Colloid Interface Sci.* 2007; 307:246–253. [PubMed: 17182054]
41. Ramanathan M, Shrestha LK, Mori T, Ji Q, Hill JP, Ariga K. *Phys. Chem. Chem. Phys.* 2013; 15:10580–10611. [PubMed: 23639971]
42. Déziel E, Lépine F, Milot S, Villemur R. *Microbiology.* 2003; 149:2005–2013. [PubMed: 12904540]
43. Römling U, Galperin MY, Gomelsky M. *Microbiol. Mol. Biol. Rev.* 2013; 77:1–52. [PubMed: 23471616]
44. Kadam RU, Bergmann M, Hurley M, Garg D, Cacciarini M, Swiderska MA, Nativi C, Sattler M, Smyth AR, Williams P, Cámara M, Stocker A, Darbre T, Reymond J-L. *Angew. Chem. Int. Ed.* 2011; 50:10631–10635.
45. Reymond J-L, Bergmann M, Darbre T. *Chem. Soc. Rev.* 2013; 42:4814–4822. [PubMed: 23370573]
46. Tomich M, Planet PJ, Figurski DH. *Nat. Rev. Micro.* 2007; 5:363–375.
47. Romero D, Aguilar C, Losick R, Kolter R. *Proc. Natl. Acad. Sci. USA.* 2010; 107:2230–2234. [PubMed: 20080671]

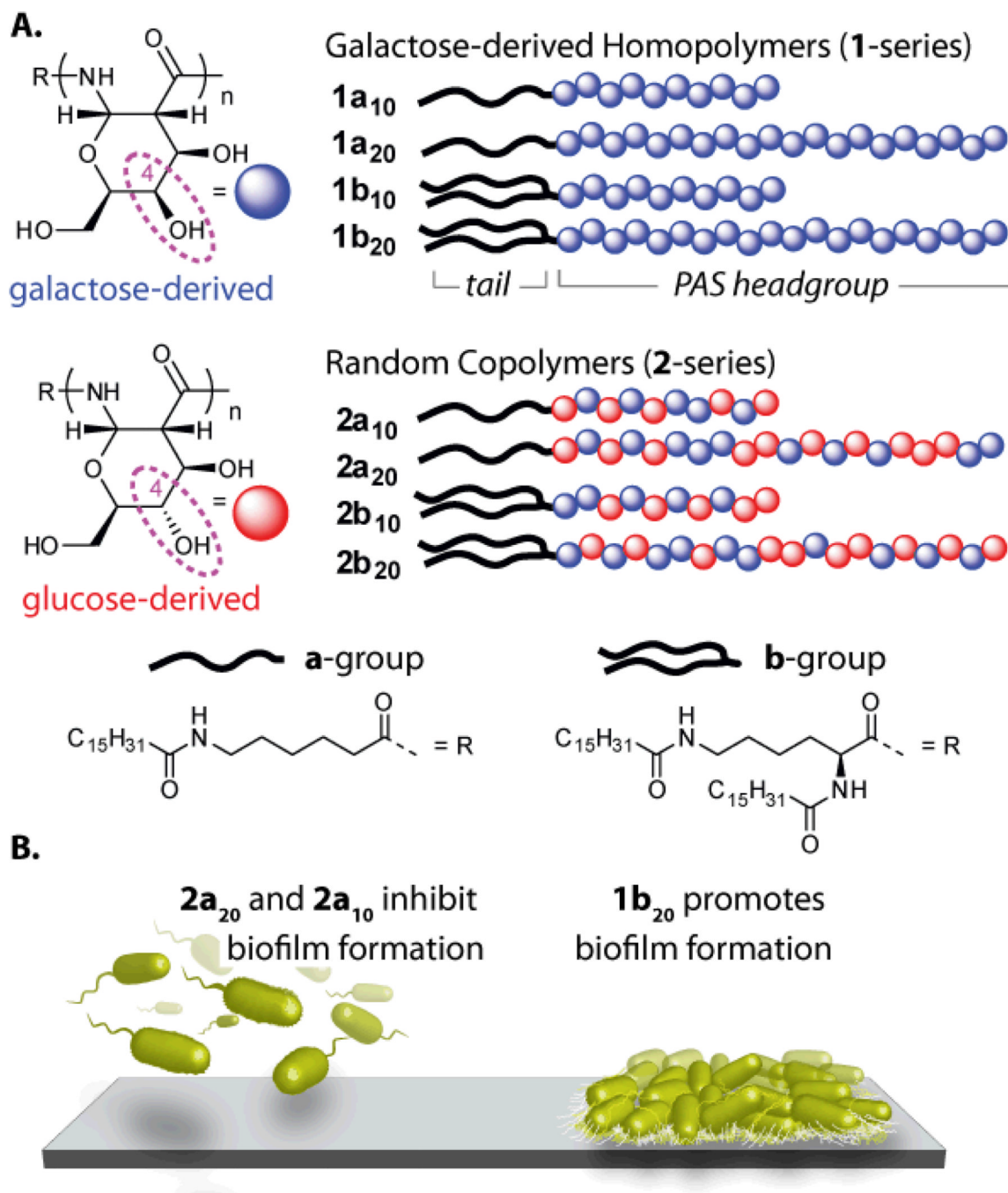
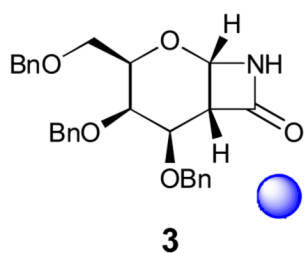
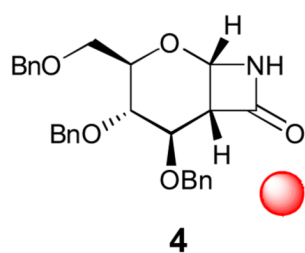


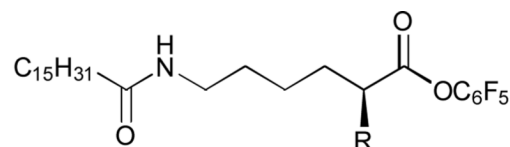
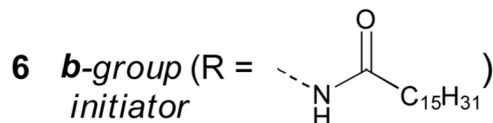
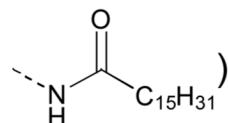
Figure 1.
A. Schematic representations of PAS amphiphiles. **B.** Cartoon of biofilm modulation showing biofilm inhibition (left) and biofilm promotion (right).



galactose-derived monomer



glucose-derived monomer

**5** a-group initiator (R = H)**6** b-group (R = ) initiator

Gal-derived Homopolymers (1-series)		initiator mol%	yield over both steps	CMC (μM)
a-group	3 + 5 X mol%	1'a₁₀ (X = 10)	1a₁₀ (75%)	<1
		1'a₂₀ (X = 5)	1a₂₀ (81%)	<1
b-group	3 + 6 X mol%	1'b₁₀ (X = 10)	1b₁₀ (81%)	<1
		1'b₂₀ (X = 5)	1b₂₀ (96%)	14
Random Copolymers (2-series)				
a-group	3/4 + 5 (1:1) X mol%	2'a₁₀ (X = 10)	2a₁₀ (73%)	20
		2'a₂₀ (X = 5)	2a₂₀ (75%)	36
b-group	3/4 + 6 (1:1) X mol%	2'b₁₀ (X = 10)	2b₁₀ (71%)	14
		2'b₂₀ (X = 5)	2b₂₀ (75%)	15

i.) LiHMDS (2.5X mol%), THF, 0 °C to rt, 1 h; ii.) Na/NH₃, -78 °C, 1 h

Figure 2.
PAS amphiphile synthesis.

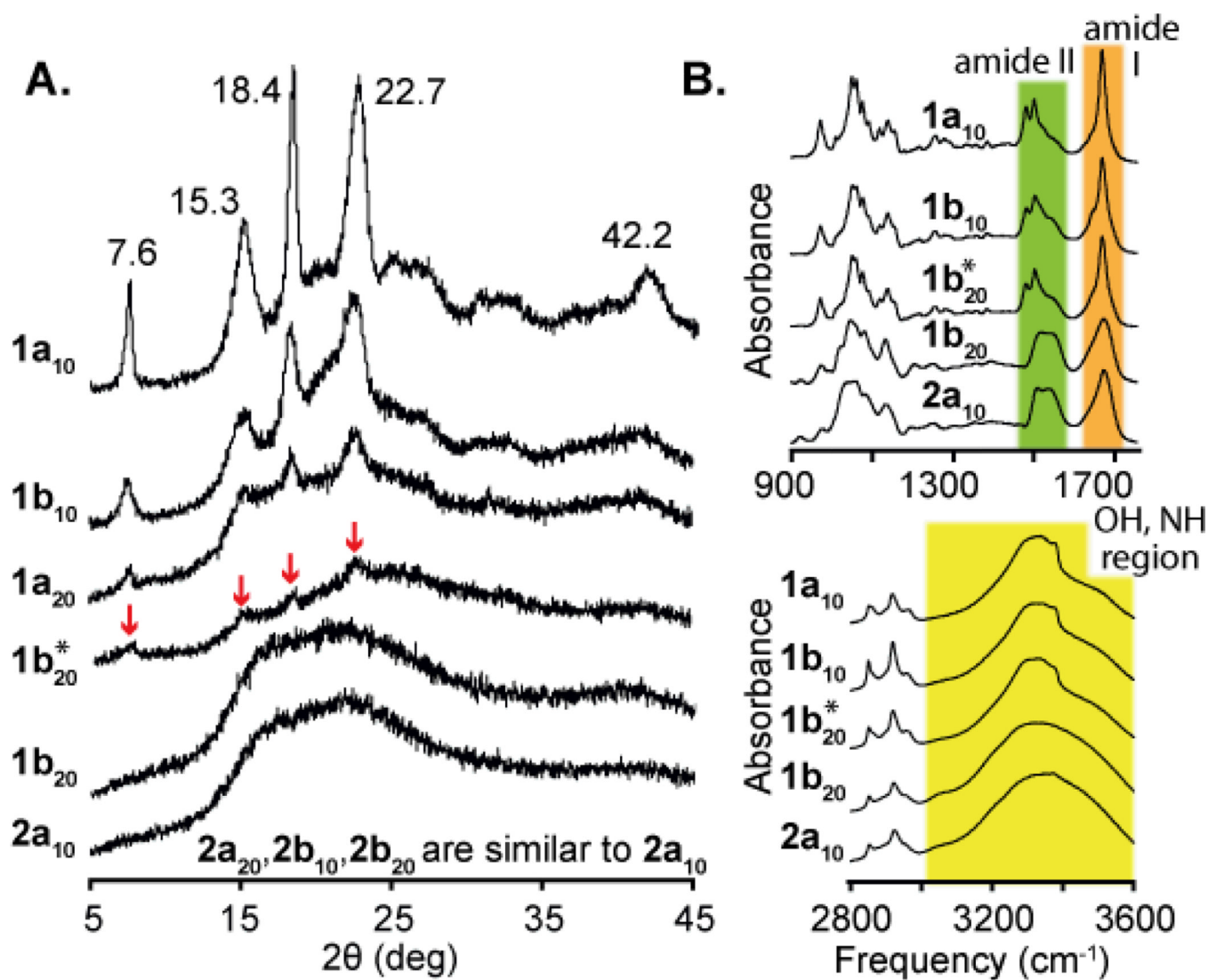


Figure 3.

A. WAXS of powder samples of amphiphiles. Sample $1b_{20}^*$ was incubated overnight at 37 °C in PBS (4 mg/mL), dialyzed, and then lyophilized. The red arrows point to the peaks suggesting increased crystalline order. **B.** IR spectra of select amphiphiles. The amide I (green), amide II (orange), and OH/NH (yellow) regions are highlighted.

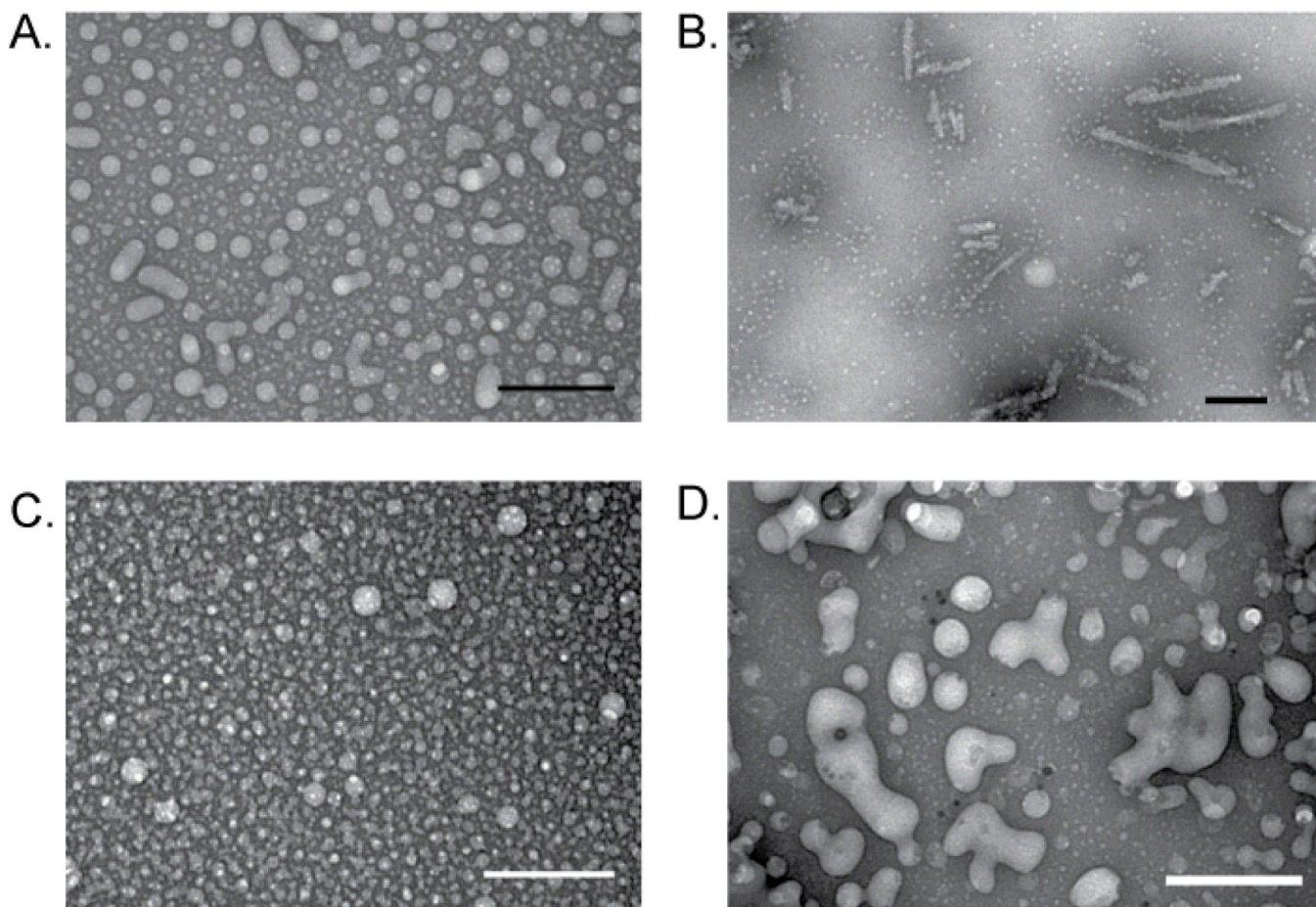


Figure 4. TEM micrographs of **1b₂₀** before (A) and after (B) incubation at 37°C for 16 hours showing the transition from globular micelles to worm-like micelles. Amphiphiles **2a₁₀** (C) and **2a₂₀** (D) appear as globular micelles by TEM. All samples were negatively stained with 1% ammonium molybdate pH 7.0 and sample concentrations were 1.0 mg/mL for A, 4.0 mg/mL for B, 2.0 mg/mL for C, and 0.8 mg/mL for D. Scale bars = 100 nm.

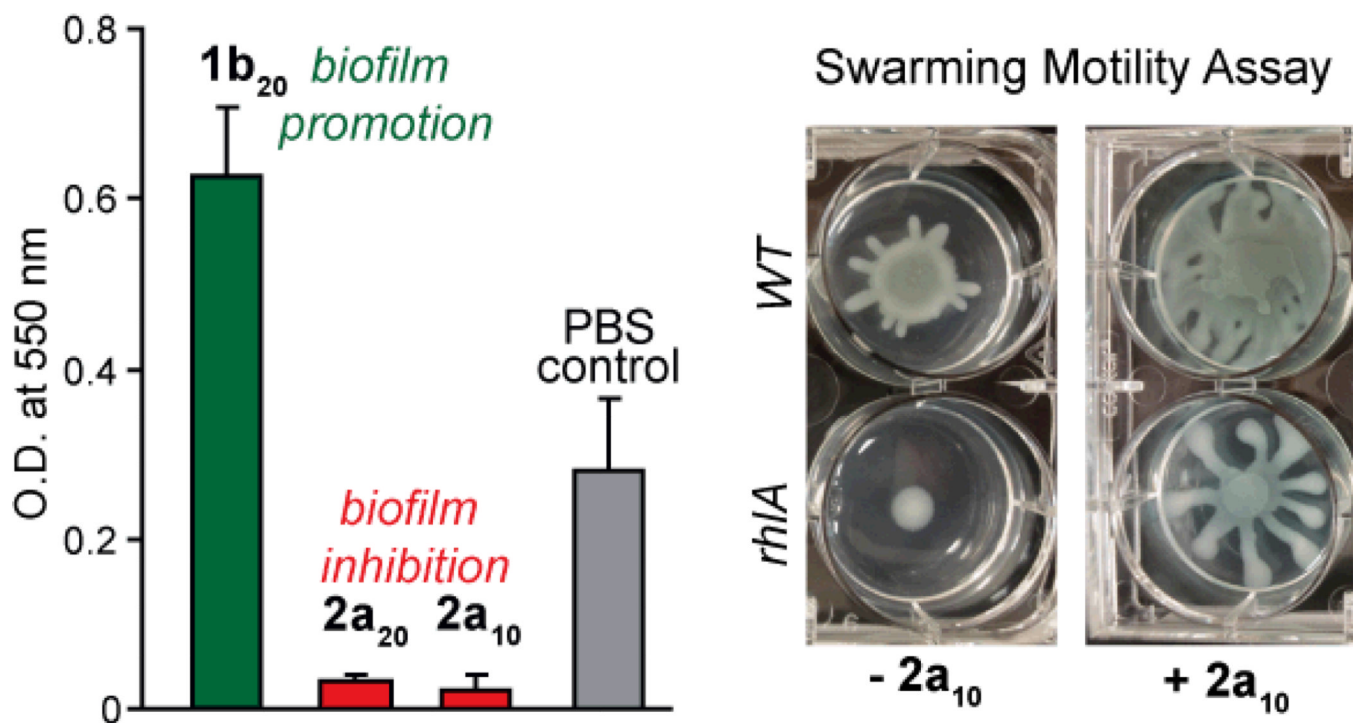


Figure 5. (bar graph) The relative amount of *P. aeruginosa* PA14 biofilm formation measured using crystal violet stain is shown for 0.5 mg/mL solutions of **1b₂₀**, **2a₁₀**, and **2a₂₀** (incubation time 8 hours, n = 3, error bars show std. dev.). (right) A swarming assay showing the effect of **2a₁₀** (0.5 mg/mL) on wild type (WT) and rhamnolipid-deficient mutant (*rhlA*) strains. Addition of **2a₁₀** restored the swarming behavior in the *rhlA* strains, a result consistent with **2a₁₀** acting as a surfactant to inhibit biofilm formation.

Table 1

Sizing of Assemblies by Dynamic Light Scattering

PAS Amphiphile ^a	D_h (nm) ^b	polydispersity
1b₂₀	34	0.29
1b₂₀* (16 h at 37°C)	105	0.25
2a₁₀	209	0.35
2a₂₀	111	0.39
2b₁₀	40	0.3
2b₂₀	80	0.35

^a Concentration 1.0 mg/mL in PBS buffer, measurements performed at 25°C.

^b Apparent hydrodynamic diameter.